



Cite this: *Phys. Chem. Chem. Phys.*, 2016, 18, 32155

Received 19th September 2016,
Accepted 1st November 2016

DOI: 10.1039/c6cp06449c

www.rsc.org/pccp

Theoretical study on σ - and π -hole carbon···carbon bonding interactions: implications in CFC chemistry†

Antonio Bauzá and Antonio Frontera*

In this manuscript the ability of CO_2 and several CFCs to establish noncovalent carbon···carbon interactions (termed as noncovalent carbon···carbon bonding) with atmospheric gases CO, ethene and ethyne has been studied at the RI-MP2/def2-TZVPD level of theory. We have used several CFCs (CFCl_3 , CF_3Cl , CF_2Cl_2 and CH_3F) and the CO_2 molecule as σ - and π -hole carbon bond donors (electron poor carbon atoms). As electron rich moieties we have used CO, ethene and ethyne (electron rich carbon atom bearing molecules). We have also used Bader's theory of "atoms in molecules" to further analyse and characterize the noncovalent interactions described herein. Finally, we have analyzed possible cooperativity effects between the noncovalent carbon···carbon bonding and hydrogen bonding interactions in the case of ethyne.

Introduction

Noncovalent interactions are recognized as key players in modern chemistry.¹ Actually, supramolecular chemists rely on their proper comprehension and rationalization in order to achieve progress in fields such as, molecular recognition^{2,3} and materials science.⁴ Hydrogen bonding and, more recently, halogen bonding are examples of well-known σ -hole interactions that play an important role in many chemical and biological environments.^{5,6} For instance, hydrogen bonding interactions are main driving forces in enzyme chemistry and protein folding.⁷ Consequently, both noncovalent forces have been widely studied from theoretical and experimental perspectives.^{8,9} Their similarities in both strength and directionality features stimulated a series of studies using the Cambridge Structural Database (CSD) in order to shed light on the impact of these interactions in crystal structures.^{10,11} Related to this, σ -hole interactions involving elements of Groups IV–VI have also earned recognition among the scientific society as an important addition to the family of well-established directional non-covalent interactions.^{12–14} Recently, it was demonstrated that atoms of Groups IV–VI (from tetrels to chalcogens) when covalently bonded are able to establish attractive interactions with electron rich entities through their positive electrostatic potential regions, which are attributed to the anisotropies of the electronic density distribution on the extensions of their covalent bonds.^{15–18}

It was also shown that the factors that rule the σ -hole potentials are the same across Groups IV–VI.

As a natural consequence of the scientific curiosity over the σ -hole chemistry a novel and relatively unexplored group of noncovalent interactions emerged, called π -hole bonding. A π -hole is a region of positive electrostatic potential that is perpendicular to a portion of a molecular framework.¹⁹ Two pioneering works that exemplify the impact of π -hole interactions in chemical and biological systems should be emphasized. Firstly, Bürgi and Dunitz studied the trajectory along which a nucleophile attacks the π -hole of a $\text{C}=\text{O}$ group^{20–22} and, secondly, Egli and co-workers studied and rationalized the ability of guanosine to behave as a π -hole donor in the crystal structure of Z-DNA.²³ More recently, the study of π -hole interactions has been extended to acyl carbons²⁴ and other entities involving pnictogen^{25–29} and chalcogen bearing compounds.^{30,31}

Haloalkanes were widely used in industry as refrigerant agents, propellants and cleaning solvents until the 1970s.³² Related to this, chlorofluorocarbons (CFCs) are a family of haloalkane compounds mostly formed by hydrocarbons, particularly alkanes, covalently bonded with halogens such as chlorine or fluorine. Nowadays, they are well known to play a key role in the depletion process of the ozone layer, which is a vital natural defense against the incoming UV radiation.³³ Several theoretical studies have been devoted to analyse the interaction between CFCs and ozone, carbon dioxide and nitrogen oxide molecules, as well as sulphur containing compounds.^{34–36} While CFCs are considered as an important source of carbon atoms,³⁷ it is intriguing whether they can undergo carbon bonding interactions with other atmospheric gases, such as carbon monoxide or ethene and ethyne molecules.^{38,39} In this regard, we propose to coin the term dicarbon bond, since both

Department of Chemistry Universitat de les Illes Balears, Ctra. de Valldemossa km 7.5, 07122 Palma, Balears, Spain. E-mail: toni.frontera@uib.es;

Fax: +34 971 173426

† Electronic supplementary information (ESI) available. See DOI: 10.1039/c6cp06449c



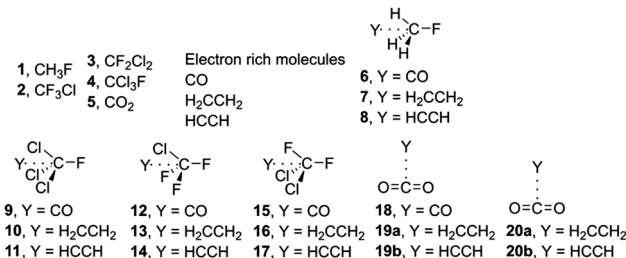


Fig. 1 Compounds **1–5** and complexes **6–20** used in this study. For complexes **19** and **20** two possible orientations were considered; parallel (denoted as a) and perpendicular (denoted as b).

the electron donor and acceptor belong are carbon atoms, thus resembling the concept of the dihydrogen bond.⁴⁰ The concept of carbon–carbon interactions involving sp and sp² carbons has been previously studied by Remya and coworkers.⁴¹

In this study, our purpose is to investigate the ability of CFCs and CO₂ moieties to establish σ - and π -hole noncovalent carbon–carbon bonding interactions. In order to achieve this goal, we have used several CFCs (CFCl₃, CCl₃F, CH₃F and CF₂Cl₂) as σ -hole carbon bond donor entities. We have used CO, ethene and ethyne as electron rich moieties (see Fig. 1). Particularly, in CO₂ π -hole complexes, we have explored two different orientations (parallel and perpendicular) between both donor and acceptor molecules. Finally, we have also used Bader's theory of "atoms in molecules" to further describe and rationalize the interactions described above.

Theoretical methods

The energies of all complexes included in this study were computed at the RI-MP2/def2-TZVPD level of theory by means of the program TURBOMOLE version 7.0.⁴² Single point calculations at the CCSD(T)/def2-TZVP level of theory have been performed in order to give reliability to the RI-MP2 method. The MEP (molecular electrostatic potential) calculations have been performed at the MP2/def2-TZVP level of theory by means of the Gaussian09 calculation package.⁴³ Frequency calculations have been performed at the RI-MP2/def2TZVPD level of theory and in all cases a true minima have been found. Moreover, all carbon–carbon complexes correspond to global minima apart from complex **8** that is a local minimum. The global minimum corresponds to an H-bonded complex CH₃F···HCCH. Bader's "Atoms in molecules" theory has been used to study the interactions discussed herein by means of the AIMall calculation package.⁴⁴ The calculations for wavefunction analyses were carried out at the MP2/def2-TZVP level of theory.

Results and discussion

MEPs study

As a preliminary study, we have computed the molecular electrostatic potential (MEP) surface of compounds **1** to **5** (see Fig. 2). As it can be observed, for compounds **1** to **4** the MEP surface showed the presence of a positive potential area located

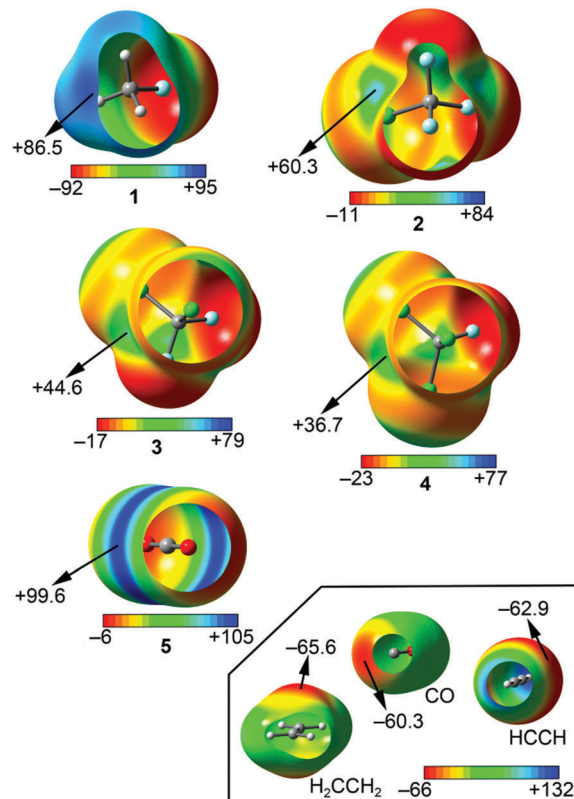


Fig. 2 MEP (molecular electrostatic potential) surfaces for compounds **1** to **5**. Energy values in kJ mol^{-1} .

at the outermost region of the carbon atom, opposite to the C–X bond (σ -hole). Consequently, an attractive interaction with electron rich entities is expected. In addition, the MEP value of the σ -hole is more positive for compounds **1** and **2**, thus expecting a stronger binding upon complexation from an electrostatic perspective. Moreover, the MEP values become less positive ongoing from compound **2** to **4**, due to the difference in electronegativity between chlorine and fluorine atoms. In the case of compound **5**, a positive potential region is observed on the tip of the carbon atom, perpendicularly located over the molecular plane (π -hole). The MEP value obtained is the most positive among compounds **1** to **5**, thus expecting a stronger binding for π -complexes over the σ -hole set. Finally, among the electron donors, the most negative MEP value corresponds to the ethene molecule, thus expecting a slightly stronger binding over the other CO and ethyne molecules.

Energetic study

The interaction energies and equilibrium distances obtained for complexes **6** to **20** (see Fig. 3) studied herein are summarized in Table 1. The examination of the results indicates that the interaction energy values are weak but attractive in all cases, ranging from -11 to -4 kJ mol^{-1} . Among the σ -hole complexes studied (**6–17**) the CFCl₃ and CF₂Cl₂ ones (**9–11** and **15–17**, respectively) present stronger interaction energies, conversely to the MEP analysis that shows more positive values at the σ -hole of CH₃F and CF₃Cl molecules likely due to the greater



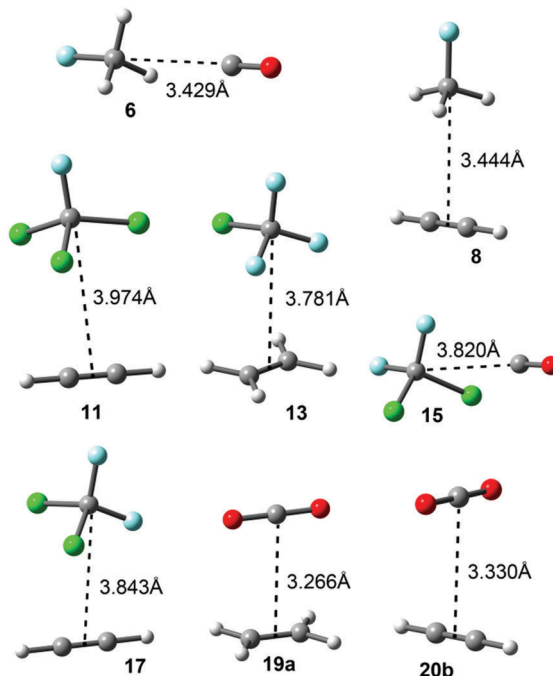


Fig. 3 Optimized geometries of some representative complexes at the RI-MP2/def2-TZVPD level of theory.

Table 1 Interaction energies (ΔE , kJ mol^{-1}), equilibrium distances (R , Å) and symmetry point groups used (Symm.) at the RI-MP2/def2-TZVPD level of theory for complexes 6 to 20

Complex	ΔE^a	R^b	Symm.
6 ($\text{OC:CH}_3\text{F}$)	-4.3	3.429	C_{3v}
7 ($\text{H}_2\text{CCH}_2:\text{CH}_3\text{F}$)	-7.0 (-6.7)	3.452	C_s
8 ($\text{HCCCH:CH}_3\text{F}$)	-6.2	3.444	C_s
9 ($\text{OC:CCl}_3\text{F}$)	-4.8 (-4.3)	3.922	C_{3v}
10 ($\text{H}_2\text{CCH}_2:\text{CCl}_3\text{F}$)	-10.8	3.937	C_s
11 ($\text{HCCH:CCl}_3\text{F}$)	-8.6	3.974	C_s
12 (OC:CClF_3)	-4.1 (-4.0)	3.748	C_s
13 ($\text{H}_2\text{CCH}_2:\text{CClF}_3$)	-7.6	3.781	C_s
14 (HCCH:CClF_3)	-6.3 (-5.5)	3.802	C_s
15 ($\text{OC:CCl}_2\text{F}_2$)	-4.5	3.820	C_s
16 ($\text{H}_2\text{CCH}_2:\text{CCl}_2\text{F}_2$)	-9.4 (-8.2)	3.830	C_s
17 ($\text{HCCH:CCl}_2\text{F}_2$)	-7.8	3.843	C_s
18 (OC:CO_2)	-5.4	3.240	C_{2v}
19a ($\text{H}_2\text{CCH}_2:\text{CO}_2$)	-9.2	3.266	C_{2v}
19b ($\text{H}_2\text{CCH}_2:\text{CO}_2$)	-8.8	3.252	C_{2v}
20a (HCCH:CO_2)	-9.8	3.210	C_{2v}
20b (HCCH:CO_2)	-6.1	3.330	C_{2v}

^a Values in parentheses correspond to the CCSD(T)/def2-TZVPD level of theory. ^b For complexes involving ethene and ethyne distances were measured from the C-C bond centroid.

polarizability of chlorine *vs.* fluorine. Moreover, CFCl_3 and CF_2Cl_2 complexes present larger equilibrium distance values than those involving CH_3F and CF_3Cl molecules. On the other hand, for CH_3F and CF_3Cl complexes (6–8 and 12–14, respectively) comparable interaction energy values were obtained. For π -complexes involving CO_2 (18 to 20b) the binding energy values are similar to those obtained for CCl_3F and CF_2Cl_2 complexes. For some complexes we have computed the interaction energies at a higher level of theory in order to validate

the computational method used herein. The values in parentheses summarized in Table 1 correspond to the interaction energies at the CCSD(T)/def2-TZVPD level of theory, which are in good agreement with the MP2 values.

The σ -hole CFC complexes with ethene (7, 10, 13, 16) are more favourable than the complexes with ethyne, in agreement with the MEP values shown in Fig. 2, which indicate that ethene is slightly more π -basic than ethyne. In addition, complexes involving the CO molecule achieved the lowest binding energy values of the set, also in agreement with the MEP analysis. For π -hole complexes 18 to 20 the parallel orientation presents larger binding energy values than the perpendicular one, likely due to a major overlap between the π -systems of CO_2 and ethene/ethyne molecules. Moreover, the $\text{CO}_2 \cdots$ ethene π -hole complexes 19a,b are more favourable than the ethyne ones (20a,b).

AIM analysis

We have used Bader's theory of "atoms in molecules" to characterize the noncovalent carbon–carbon bond complexes described above. The distribution of critical points (CPs) and bond paths for some representative complexes is shown in Fig. 4. For σ -hole complexes involving the CH_3F moiety (6 to 8) the presence of a bond CP (red sphere) and bond path (dashed line) connecting both carbon atoms can be noted. In addition, in the case of complex 7 two symmetrically distributed bond CPs connect the π -system of ethene (both C atoms) to the carbon atom of the CH_3F moiety, consequently a supramolecular ring is formed and a ring CP is created. On the other hand, for complexes involving the CO_2 moiety (18, 19b and 20b)

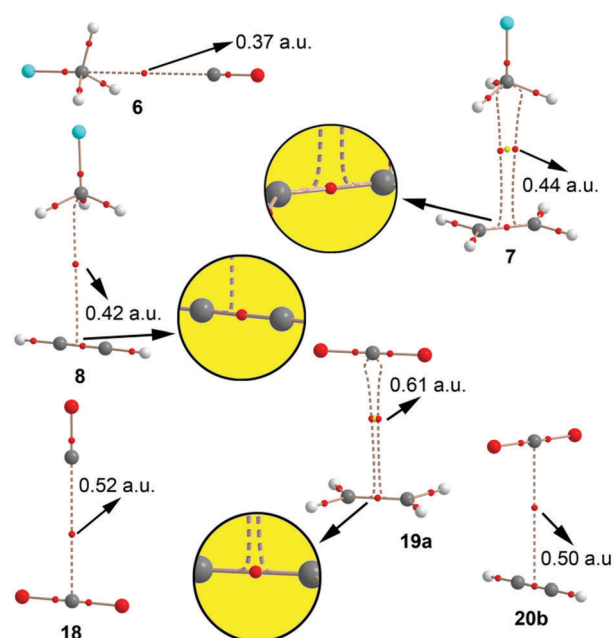


Fig. 4 Distribution of critical points and bond paths in complexes 6, 7, 8, 18, 19a and 20b. Bond and ring critical points are represented by red and yellow spheres, respectively. The bond paths connecting bond critical points are also represented. The value of the density at the bond critical point ($\rho \times 10^2$) is also indicated.

the interaction is characterized by the presence of a bond CP and bond path connecting the carbon atom of CO_2 to either the carbon atom of CO or the bond critical point of the CC bond of ethene/ethyne. Moreover, in complex **19a** where the CO_2 and the ethene portions are disposed in parallel, the presence of two symmetrically distributed bond CPs connecting both C atoms of the ethene to the central C atom of CO_2 can be noted, forming a supramolecular ring and its corresponding ring CP. The values of the Laplacian are all positive, as in common in closed shell calculations. Finally, additional AIM analyses are included in the ESI† (see Fig. S1). In these complexes the bond paths that characterize the interaction connect the carbon atoms of the electron rich molecules to the halogen atoms of the CFCs.

Noncovalent carbon–carbon bonding vs. H-bonding

This manuscript is devoted to the ability of CFCs to establish noncovalent carbon–carbon bonding with other atmospheric gases. It should be mentioned that the most favourable binding mode between CH_3F and ethyne is the formation of a hydrogen-bonded complex by means of a $\text{HCC}-\text{H}\cdots\text{FCH}_3$ interaction. The interaction energy of the global minimum is -8.8 kJ mol^{-1} while the carbon–carbon complex **8** is -6.2 kJ mol^{-1} . We have also analysed possible cooperativity effects between both interactions. Particularly, we have computed the binding energies of ethyne interacting with two CH_3F molecules either forming two H-bonds (ΔE_1 , complex **21**) or two noncovalent carbon–carbon bonds (ΔE_2 , complex **22**), see Fig. 5. It can be observed that the H-bonding complex is approximately 5 kJ mol^{-1} more favourable than the noncovalent carbon–carbon complex. More interestingly, the H-bonded complex **21** has enhanced the ability to interact with additional CH_3F molecules forming noncovalent carbon–carbon bonding interactions ($\Delta E_3 = -19.8 \text{ kJ mol}^{-1}$) to form complex **23**. Similarly, the noncovalent carbon–carbon bonded complex **22** forms stronger H-bonding interactions

($\Delta E_4 = -24.7 \text{ kJ mol}^{-1}$) than ethyne alone ($\Delta E_1 = -16.5 \text{ kJ mol}^{-1}$). Therefore, strong cooperativity effects are found between both interactions in the formation of complex **23**. This mutual influence between the interactions is further confirmed by the AIM analysis. The charge density at the bond CP is usually related to the interaction strength.⁴⁵ It can be observed that the values of $\rho(r)$ at the bond CPs that characterize the H-bonding and noncovalent carbon–carbon bonding interactions in complex **23** are greater than the corresponding values in complexes **21** and **22**, thus confirming the mutual reinforcement of both interactions, in agreement with the energetic study (Fig. 5).

Conclusions

The results reported in this manuscript highlight the ability of CFCs and CO_2 molecules to establish weak interactions (noncovalent carbon–carbon bonds) with CO, ethene and ethyne molecules acting as electron donors, which are present in the higher layers of the atmosphere. The results presented herein provide new insights into how these molecules interact with each other and may be important in the field of atmospheric chemistry. We have successfully used Bader's theory of "atoms in molecules" to characterize the noncovalent carbon–carbon bond complexes described above. Finally, favourable cooperativity effects between noncovalent carbon–carbon and hydrogen bonding interactions have been demonstrated energetically using the AIM theory.

Acknowledgements

A. B. and A. F. thank the DGICYT of Spain (projects CTQ2014-57393-C2-1-P and CONSOLIDER INGENIO 2010 CSD2010-00065, FEDER funds). We thank the CTI (UIB) for computational facilities.

References

Figure 5 shows the distribution of critical points and bond paths in complexes **21**–**23**, along with the binding energies. The value of the density at the bond critical point is also indicated in italics.

- 1 C. A. Hunter and J. K. M. Sanders, *J. Am. Chem. Soc.*, 1990, **112**, 5525.
- 2 H. J. Schneider, *Angew. Chem., Int. Ed.*, 2009, **48**, 3924.
- 3 C. A. Hunter and J. K. M. Sanders, *J. Am. Chem. Soc.*, 1990, **112**, 5525.
- 4 W. J. Vickaryous, R. Herges and D. W. Jonhson, *Angew. Chem., Int. Ed.*, 2004, **43**, 5831.
- 5 S. J. Grabowski, *Chem. Rev.*, 2011, **111**, 2597.
- 6 P. Murrayrust and W. D. S. Motherwell, *J. Am. Chem. Soc.*, 1979, **101**, 4374.
- 7 Y. Bai, T. R. Sosnick, L. Mayne and S. W. Englander, *Science*, 1995, **269**, 192.
- 8 A. C. Legon and D. J. Millen, *Acc. Chem. Res.*, 1987, **20**, 39.
- 9 P. Metrangolo, H. Neukirch, T. Pilati and G. Resnati, *Acc. Chem. Res.*, 2005, **38**, 386.
- 10 G. A. Cavallo, P. Metrangolo, R. Milani, T. Pilati, A. Priimagi, G. Resnati and G. Terraneo, *Chem. Rev.*, 2016, **116**, 2478.
- 11 T. Steiner, *Angew. Chem., Int. Ed.*, 2002, **41**, 48.

Fig. 5 Distribution of critical points and bond paths in complexes **21**–**23**, along with the binding energies. The value of the density at the bond critical point is also indicated in italics.



12 P. Politzer, J. S. Murray and T. Clark, *Phys. Chem. Chem. Phys.*, 2010, **12**, 7748.

13 K. E. Riley, J. S. Murray, J. Franfrlík, J. Rezáč, R. J. Solá, M. C. Concha, F. M. Ramos and P. Politzer, *J. Mol. Model.*, 2011, **17**, 3309.

14 A. Bauzá, T. J. Mooibroek and A. Frontera, *Angew. Chem., Int. Ed.*, 2013, **52**, 12317.

15 S. C. Nyburg and C. H. Faerman, *Acta Crystallogr., Sect. B: Struct. Sci.*, 1985, **41**, 274.

16 P. Politzer, K. E. Riley, F. A. Bulat and J. S. Murray, *Comput. Theor. Chem.*, 2012, **998**, 2.

17 T. N. G. Row and R. Parthasarathy, *J. Am. Chem. Soc.*, 1981, **103**, 477.

18 N. Ramasubbu and R. Parthasarathy, *Phosphorus Sulfur Relat. Elem.*, 1987, **31**, 221.

19 J. S. Murray, P. Lane, T. Clark, K. E. Riley and P. Politzer, *J. Mol. Model.*, 2012, **18**, 541.

20 H. B. Burgi, *Inorg. Chem.*, 1973, **12**, 2321.

21 H. B. Burgi, J. D. Dunitz and E. Shefter, *J. Am. Chem. Soc.*, 1973, **95**, 5065.

22 H. B. Burgi, J. D. Dunitz, J. M. Lehn and G. Wipff, *Tetrahedron*, 1974, **30**, 1563.

23 M. Egli and R. V. Gessner, *Proc. Natl. Acad. Sci. U. S. A.*, 1995, **92**, 180.

24 P. Sjoberg and P. Politzer, *J. Phys. Chem.*, 1990, **94**, 3959.

25 A. Bauzá, R. Ramis and A. Frontera, *J. Phys. Chem. A*, 2014, **118**, 2827.

26 A. Bauzá, T. J. Mooibroek and A. Frontera, *Chem. Commun.*, 2015, **51**, 1491.

27 A. Bauzá, A. Frontera and T. J. Mooibroek, *Cryst. Growth Des.*, 2016, **16**, 5520.

28 A. Bauzá, T. J. Mooibroek and A. Frontera, *Chem. Commun.*, 2015, **51**, 1491.

29 A. Bauzá, T. J. Mooibroek and A. Frontera, *ChemPhysChem*, 2016, **17**, 1608.

30 L. M. Azofra, I. Alkorta and S. Scheiner, *Theor. Chem. Acc.*, 2014, **133**, 1586.

31 L. M. Azofra, I. Alkorta and S. Scheiner, *Phys. Chem. Chem. Phys.*, 2014, **16**, 18974.

32 A. Chatterjee, T. Ebina, T. Iwasaki and F. Mizukami, *J. Mol. Struct.*, 2003, **630**, 233.

33 J. E. Lovelock, R. J. Maggs and R. A. Rasmussen, *Nature*, 1972, **237**, 452.

34 B. G. de Oliveira, R. C. M. Ugulino de Araújo, E. S. Leite and M. N. Ramos, *Int. J. Quantum Chem.*, 2011, **111**, 111.

35 K. S. Diao, F. Wang and H. J. Wang, *J. Mol. Struct.*, 2009, **913**, 195.

36 L. Ai and J. Liu, *J. Mol. Model.*, 2014, **20**, 2179.

37 K. S. Diao, F. Wang and H. J. Wang, *Bull. Environ. Contam. Toxicol.*, 2010, **84**, 170.

38 J. G. Calvert, R. Atkinson, J. A. Kerr, S. Madronich, G. K. Moortgat and T. J. Wallington, *et al.*, The Mechanisms of Atmospheric Oxidation of the Alkenes, Oxford University Press, New York, 2000.

39 (a) M. P. Fraser, G. R. Cass and B. R. Simoneit, *Environ. Sci. Technol.*, 1998, **32**, 2051; (b) A. C. Aikin, J. R. Herman, E. J. Maier and C. J. McQuillan, *J. Geophys. Res.*, 1982, **87**, 3105; (c) Y. Xiaoi, D. J. Jacob and S. Turquety, *J. Geophys. Res.*, 2007, **112**, D12305.

40 R. Custelcean and J. E. Jackson, *Chem. Rev.*, 2001, **101**, 1963.

41 K. Remya and C. H. Suresh, *Phys. Chem. Chem. Phys.*, 2015, **17**, 18380.

42 R. Ahlrichs, M. Bär, M. Hacer, H. Horn and C. Kömel, *Chem. Phys. Lett.*, 1989, **162**, 165.

43 M. J. Frisch, G. W. Trucks, H. B. Schlegel, G. E. Scuseria, M. A. Robb, J. R. Cheeseman, G. Scalmani, V. Barone, B. Mennucci, G. A. Petersson, H. Nakatsuji, M. Caricato, X. Li, H. P. Hratchian, A. F. Izmaylov, J. Bloino, G. Zheng, J. L. Sonnenberg, M. Hada, M. Ehara, K. Toyota, R. Fukuda, J. Hasegawa, M. Ishida, T. Nakajima, Y. Honda, O. Kitao, H. Nakai, T. Vreven, J. A. Montgomery, Jr., J. E. Peralta, F. Ogliaro, M. Bearpark, J. J. Heyd, E. Brothers, K. N. Kudin, V. N. Staroverov, R. Kobayashi, J. Normand, K. Raghavachari, A. Rendell, J. C. Burant, S. S. Iyengar, J. Tomasi, M. Cossi, N. Rega, J. M. Millam, M. Klene, J. E. Knox, J. B. Cross, V. Bakken, C. Adamo, J. Jaramillo, R. Gomperts, R. E. Stratmann, O. Yazyev, A. J. Austin, R. Cammi, C. Pomelli, J. W. Ochterski, R. L. Martin, K. Morokuma, V. G. Zakrzewski, G. A. Voth, P. Salvador, J. J. Dannenberg, S. Dapprich, A. D. Daniels, Ö. Farkas, J. B. Foresman, J. V. Ortiz, J. Cioslowski and D. J. Fox, *Gaussian 09, Revision B.01*, Gaussian, Inc., Wallingford CT, 2009.

44 T. A. Keith, *AIMAll (Version 13.05.06)*, TK Gristmill Software, Overland Park KS, USA, 2013.

45 J. Leszczynski, in *Computational Chemistry: Reviews of Current Trends*, ed. J. Leszczynski, World Scientific, Singapore, 1996, vol. 4.

